Mon. Not. R. astr. Soc. (1986) **221**, 1001–1022

Mass models with Stäckel potentials

Tim de Zeeuw *Institute for Advanced Study, Princeton, NJ 08540, USA*
Reynier Peletier★ and Marijn Franx *Sterrewacht Leiden, Postbus 9513, 2300 RA Leiden, The Netherlands*

Accepted 1986 April 7. Received 1986 April 7; in original form 1986 February 24

Summary. Triaxial mass models with a gravitational potential of Stäckel form in ellipsoidal coordinates are investigated. Models are constructed by specification of the z-axis density profile $\psi(z)$, choice of an ellipsoidal coordinate system, and subsequent application of the generalized Kuzmin formula.

For each profile $\psi(z)$ there is a two-parameter family of triaxial separable models. The parameters are the positions of the two pairs of foci on the z-axis of the ellipsoidal coordinates in which the potential is of Stäckel form or, equivalently, the central axis ratios of the density distribution. Smooth mass models are generated by smooth profiles $\psi(z)$. The density, ϱ, in these separable models cannot fall off more rapidly than r^{-4} as the radius $r \to \infty$, except on the z-axis. All models in which ϱ falls off less rapidly than r^{-4} become round as $r \to \infty$. Models with a singular density in the centre only do not exist.

Specific examples are presented. Among these is a separable triaxial generalization of the modified Hubble model $[\varrho \sim (1+r^2)^{-3/2}]$. For a number of cases the potential is given explicitly.

1 Introduction

Many triaxial mass models exist in which all stellar orbits enjoy three exact isolating integrals of motion. The gravitational potential of these models is of Stäckel form, so that the Hamilton–Jacobi equation is separable in ellipsoidal coordinates. Such separable mass models are especially valuable for a study of the dynamics of elliptical galaxies (de Zeeuw 1985a, hereafter Paper I; see also Gerhard 1985). The orbits in them are nearly identical to the orbits found in the numerical self-consistent models of triaxial galaxies, constructed by Schwarzschild (1979, 1982) and by Wilkinson & James (1982). The advantage of mass models with a Stäckel potential is that the orbits – and hence the dynamics – can be described by essentially analytic means.

Kuzmin (1956) has already studied oblate axisymmetric models of this kind. He showed that

★Present address: Kapteyn Laboratorium, Postbus 800, 9700 AV Groningen, The Netherlands.

the density at a general point is related to the density on the symmetry axis by a simple formula. He proved that the density is nowhere negative if it is non-negative on the symmetry axis. This is Kuzmin's theorem.

In Paper II (de Zeeuw 1985b) we generalized Kuzmin's formula, and his theorem, to triaxial mass models with a Stäckel potential. This led to a new method for the construction of such models. First one chooses a density profile and an ellipsoidal coordinate system. One integration then produces, via the generalized Kuzmin formula, the complete mass model that has a potential of Stäckel form in the chosen coordinates. The potential can be calculated explicitly by one more, straightforward, integration.

In the present paper we construct by this method a number of separable mass models for simple density profiles, and show that these give rise to smooth three-dimensional mass models. Our aim is to obtain insight into the variety of mass models that allow three exact isolating integrals of motion for all orbits in them, and to deduce some of their general properties. A second reason for a study of the Stäckel models is that they can be used as building blocks for more general mass models. Since the density and the potential are each determined by a function of one variable only, the extensive tabulations that are often required for the description of general triaxial mass models can be avoided.

It has recently come to our attention that – not surprisingly – some of the results presented in Papers I and II had already been obtained by Kuzmin (1973). In a brief conference contribution he presents the prototypical Stäckel model (i.e. the perfect ellipsoid of Paper I), mentions that it supports four families of general orbits, and gives the generalization of his axisymmetric formula for the density. As far as we are aware, he did not construct other triaxial mass models.

In Section 2 we outline our notation and summarize some basic results. General properties of the Stäckel models are studied in Section 3. In Section 4 we discuss expansions of the density and the potential near the centre. The reader who is not interested in the mathematical preliminaries may want to turn his attention directly to Sections 5 and 6 where we present a number of smooth Stäckel models.

2 Definitions and fundamental relations

The general Stäckel potentials lead to equations of motion that are separable in ellipsoidal coordinates (e.g. Morse & Feshbach 1953). The corresponding mass models are all triaxial. The limiting cases of separability in oblate and prolate spheroidal coordinates lead to axisymmetric mass models.

2.1 TRIAXIAL MODELS

Let (x, y, z) be Cartesian coordinates. We define ellipsoidal coordinates (λ, μ, ν) as the three roots for τ of

$$\frac{x^2}{\tau+\alpha}+\frac{y^2}{\tau+\beta}+\frac{z^2}{\tau+\gamma}=1, \tag{1}$$

where α, β and γ are constants, and $-\gamma\leq\nu\leq-\beta\leq\mu\leq-\alpha\leq\lambda$. The coordinate surfaces are ellipsoids (λ) and hyperboloids of one (μ) and two (ν) sheets. There are two pairs of foci on the z-axis, at $z=\pm\Delta_1$ and at $z=\pm\Delta_2$, and one pair on the y-axis at $y=\pm\sqrt{\Delta_2^2-\Delta_1^2}$, with $\Delta_1^2=\gamma-\beta$ and $\Delta_2^2=\gamma-\alpha$, so that $\Delta_2^2-\Delta_1^2=\beta-\alpha$. Further properties of ellipsoidal coordinates may be found in Paper I.

2.1.1 Density

For mass models with a Stäckel potential, the density at a point (λ, μ, ν) is related to the density on the z-axis by a generalized version of Kuzmin's formula (Paper II). The z-axis is given by

$$\begin{aligned} &\lambda=-\alpha, \quad \mu=-\beta, \quad \nu=z^2-\gamma, \quad \text{for } 0\leq|z|\leq\Delta_1,\\ &\lambda=-\alpha, \quad \nu=-\beta, \quad \mu=z^2-\gamma, \quad \text{for } \Delta_1\leq|z|\leq\Delta_2,\\ &\mu=-\alpha, \quad \nu=-\beta, \quad \lambda=z^2-\gamma, \quad \text{for } \Delta_2\leq|z|. \end{aligned} \tag{2}$$

Let $\psi(\tau)$ be the density on the z-axis ($\tau=z^2-\gamma$; $\tau=\lambda, \mu, \nu$). Then

$$\varrho(\lambda, \mu, \nu)=g_\lambda^2\psi(\lambda)+g_\mu^2\psi(\mu)+g_\nu^2\psi(\nu)$$
$$+2g_\lambda g_\mu \frac{[\Psi(\lambda)-\Psi(\mu)]}{(\lambda-\mu)}+2g_\mu g_\nu \frac{[\Psi(\mu)-\Psi(\nu)]}{(\mu-\nu)}+2g_\nu g_\lambda \frac{[\Psi(\nu)-\Psi(\lambda)]}{(\nu-\lambda)}, \tag{3}$$

with

$$\Psi(\tau)=\int_{-\gamma}^{\tau}\psi(\sigma)\,d\sigma, \tag{4}$$

and

$$g_\lambda=\frac{(\lambda+\alpha)(\lambda+\beta)}{(\lambda-\mu)(\lambda-\nu)}, \qquad g_\mu=\frac{(\mu+\alpha)(\mu+\beta)}{(\mu-\nu)(\mu-\lambda)}, \qquad g_\nu=\frac{(\nu+\alpha)(\nu+\beta)}{(\nu-\lambda)(\nu-\mu)}, \tag{5}$$

so that $g_\lambda\geq0$, $g_\mu\geq0$, $g_\nu\geq0$ and $g_\lambda+g_\mu+g_\nu=1$. It follows immediately that a separable $\varrho(\lambda, \mu, \nu)$ is nowhere negative if, and only if, $\psi(\tau)\geq0$ for all $\tau\geq-\gamma$. This is the generalization of Kuzmin's theorem.

For a given density profile $\psi(z)$, a choice of Δ_1 and Δ_2 defines the positions of two pairs of foci on the z-axis, and thereby fixes an ellipsoidal coordinate system, so that $\psi(\tau)$ can be determined. The complete mass model that has a Stäckel potential in these coordinates then follows from (3). As a result, *for a given* $\psi(z)$ *there exists a two-parameter family of separable mass models, the parameters being* Δ_1 *and* Δ_2. All these models have reflection symmetry with respect to the three principal planes $x=0$, $y=0$ and $z=0$, i.e. they are triaxial.

We remark that if $\psi(\tau)$ is n times differentiable, then so is ϱ, except on the ellipse $\lambda=\mu=-\alpha$ in the (y,z)-plane and on the hyperbola $\mu=\nu=-\beta$ in the (x,z)-plane, where ϱ is $n-1$ times differentiable (*cf.* Lynden-Bell 1962).

The total mass M of a model can be expressed as a single integral over $\psi(\tau)$, and is easily evaluated [Paper II, equation (36)].

2.1.2 Principal planes

The generalized Kuzmin formula (3) simplifies in the three principal planes. The (y,z)-plane is given by $\mu=-\alpha$ or $\lambda=-\alpha$ (Paper I). The ellipsoidal coordinates become elliptic coordinates $(\varkappa,\nu)$ with foci at $z=\pm\Delta_1$ $(\varkappa=\lambda, \mu)$. We find

$$\varrho_{x=0}(\varkappa, \nu)=\frac{(\varkappa+\beta)^2}{(\varkappa-\nu)^2}\psi(\varkappa)+\frac{2(\varkappa+\beta)(\nu+\beta)}{(\varkappa-\nu)(\nu-\varkappa)}\frac{[\Psi(\varkappa)-\Psi(\nu)]}{(\varkappa-\nu)}+\frac{(\nu+\beta)^2}{(\nu-\varkappa)^2}\psi(\nu). \tag{6}$$

The (x, z)-plane is given by $\mu=-\beta$ or $\nu=-\beta$. The ellipsoidal coordinates reduce to elliptic coordinates (λ, σ), with foci at $z=\pm\Delta_2(\sigma=\mu, \nu)$. We obtain

$$\varrho_{y=0}(\lambda, \sigma)=\frac{(\lambda+\alpha)^2}{(\lambda-\sigma)^2}\psi(\lambda)+\frac{2(\lambda+\alpha)(\sigma+\alpha)}{(\lambda-\sigma)(\sigma-\lambda)}\frac{[\Psi(\lambda)-\Psi(\sigma)]}{(\lambda-\sigma)}+\frac{(\sigma+\alpha)^2}{(\sigma-\lambda)^2}\psi(\sigma). \tag{7}$$

The (x, y)-plane has $\nu=-\gamma$. In this plane (λ, μ) are elliptic coordinates with foci at $y=\pm\sqrt{\Delta_2^2-\Delta_1^2}$. Whereas, via (3), the z-axis density profile $\psi(\tau)$ determines the density in the (x, y)-plane, we may also express it in terms of the profile $\xi(\varkappa)$ along the y-axis ($\varkappa+\beta=y^2$, $\varkappa=\lambda, \mu$). We find

$$\xi(\varkappa)=\frac{(\varkappa+\beta)^2}{(\varkappa+\gamma)^2}\psi(\varkappa)+\frac{2(\gamma-\beta)(\varkappa+\beta)}{(\varkappa+\gamma)^3}\Psi(\varkappa)+\frac{(\gamma-\beta)^2}{(\varkappa+\gamma)^2}\psi(-\gamma). \tag{8}$$

Then we may write

$$\varrho_{z=0}(\lambda, \mu)=\frac{(\lambda+\alpha)^2}{(\lambda-\mu)^2}\xi(\lambda)+\frac{2(\lambda+\alpha)(\mu+\alpha)}{(\lambda-\mu)(\mu-\lambda)}\frac{[\Xi(\lambda)-\Xi(\mu)]}{(\lambda-\mu)}+\frac{(\mu+\alpha)^2}{(\mu-\lambda)^2}\xi(\mu), \tag{9}$$

where we have defined

$$\Xi(\varkappa)=\int_{-\beta}^{\varkappa}\xi(\sigma)\,d\sigma=\frac{(\varkappa+\beta)^2}{(\varkappa+\gamma)^2}\Psi(\varkappa)+(\gamma-\beta)\,\psi(-\gamma)\frac{(\varkappa+\beta)}{(\varkappa+\gamma)}. \tag{10}$$

It is evident that equations (6), (7) and (9) have the same form. The density – $\psi(\tau)$ or $\xi(\tau)$ – along the axis that contains the foci of the elliptic coordinates, together with the position of the foci, determines the density elsewhere in the plane. As a result, we may often obtain an impression of the shape of a triaxial mass model by inspection of the density distribution in one principal plane only. We shall see in Section 2.3 that the density in the meridional plane of an axisymmetric model is governed by a relation similar to (6), (7) or (9).

2.1.3 *Potential*

The gravitational potential of a mass model defined by (3), and a given $\psi(\tau)$, is of Stäckel form and may be written as

$$V=V_S=g_\lambda U(\lambda)+g_\mu U(\mu)+g_\nu U(\nu), \tag{11}$$

where $U(\tau)$ is the potential along the z-axis. For a given density profile $\psi(\tau)$ we can find $U(\tau)$ from the expression

$$U(\tau)=-\frac{(\tau+\gamma)\,G(\tau)-(\gamma-\beta)\,G(-\beta)}{\tau+\beta}, \tag{12}$$

where the function $G(\tau)$ is given explicitly in terms of $\psi(\tau)$ in equation (35) of Paper II. $G(\tau)$ is the function that is most convenient to use in the investigation of orbits in Stäckel potentials (Paper I). Due to the fact that the Hamilton–Jacobi equation separates in these potentials the equations of motion can be solved by a straightforward quadrature. The forcefield ∇V_S does not enter the calculations explicitly.

2.1.4 *Forces*

The separable mass models are useful building blocks for more general mass models, since both density and potential are determined by a function of one variable only. When different separable mass models are added, or when figure rotation is introduced, the resulting mass models will generally have a non-integrable Hamiltonian. Accordingly, the orbits have to be found by numerical integration of the equations of motion. This is usually done in Cartesian coordinates, and requires knowledge of the force field. We briefly show how to calculate the Cartesian components of ∇V_S.

We have

$$\left(\frac{\partial V}{\partial x}, \frac{\partial V}{\partial y}, \frac{\partial V}{\partial z}\right) = \frac{\partial(\lambda, \mu, \nu)}{\partial(x, y, z)} \left(\frac{\partial V}{\partial \lambda}, \frac{\partial V}{\partial \mu}, \frac{\partial V}{\partial \nu}\right). \tag{13}$$

By using the relations between (λ, μ, ν) and (x, y, z) given in equations (8) and (9) of Paper I we find

$$\frac{\partial(\lambda, \mu, \nu)}{\partial(x, y, z)} = \begin{pmatrix} \frac{x}{2(\lambda+\alpha)P^2} & \frac{x}{2(\mu+\alpha)Q^2} & \frac{x}{2(\nu+\alpha)R^2} \\ \frac{y}{2(\lambda+\beta)P^2} & \frac{y}{2(\mu+\beta)Q^2} & \frac{y}{2(\nu+\beta)R^2} \\ \frac{z}{2(\lambda+\gamma)P^2} & \frac{z}{2(\mu+\gamma)Q^2} & \frac{z}{2(\nu+\gamma)R^2} \end{pmatrix} \tag{14}$$

where the metric coefficients P, Q and R are given in equation (10) of Paper I.

For a Stäckel potential V_S we can express $\partial V_S/\partial\lambda$, $\partial V_S/\partial\mu$, $\partial V_S/\partial\nu$ explicitly in terms of $U(\tau)$ and its first derivative. We find

$$\frac{\partial V_S}{\partial \lambda} = g_\lambda U'(\lambda) + g_\mu \frac{[U(\lambda)-U(\mu)]}{\lambda-\mu} + g_\nu \frac{[U(\lambda)-U(\nu)]}{\lambda-\nu},$$

$$\frac{\partial V_S}{\partial \mu} = g_\lambda \frac{[U(\mu)-U(\lambda)]}{\mu-\lambda} + g_\mu U'(\mu) + g_\nu \frac{[U(\mu)-U(\nu)]}{\mu-\nu},$$

$$\frac{\partial V_S}{\partial \nu} = g_\lambda \frac{[U(\nu)-U(\lambda)]}{\nu-\lambda} + g_\mu \frac{[U(\nu)-U(\mu)]}{\nu-\mu} + g_\nu U'(\nu), \tag{15}$$

and g_λ, g_μ and g_ν are given in (5).

2.2 OBLATE SPHEROIDAL COORDINATES

For $\gamma=\beta$ we have $\Delta_1=0$ and the ellipsoidal coordinates reduce to oblate spheroidal coordinates (λ, μ, χ) that have the x-axis as symmetry axis (Paper I). Let $(x, \tilde{z}, \chi)$ be cylindrical coordinates with $\tilde{z}^2=y^2+z^2$. In each meridional plane χ=constant, λ and μ are elliptic coordinates with foci at $x=0$, $|\tilde{z}|=\Delta_2$.

In this limit, $\psi(\tau)$ is the density along the $\tilde{z}$-axis ($\tilde{z}^2=\tau+\beta$; $\tau=\lambda,\mu$), i.e. it is the density profile in the equatorial plane. Formula (3) (with $\nu=-\gamma=-\beta$) defines an axisymmetric mass model. The density at a general point is given by

$$\varrho(\lambda, \mu) = g_\lambda^2 \psi(\lambda) + 2 g_\lambda g_\mu \frac{[\Psi(\lambda)-\Psi(\mu)]}{\lambda-\mu} + g_\mu^2 \psi(\mu), \tag{16}$$

with

$$g_\lambda = \frac{\lambda+\alpha}{\lambda-\mu}, \qquad g_\mu = \frac{\mu+\alpha}{\mu-\lambda}. \tag{17}$$

A choice of Δ_2 defines an oblate spheroidal coordinate system. It is evident that for a given $\psi(\tilde{z})$ there exists a *one-parameter family* of mass models that have a potential of Stäckel form in these coordinates. All these models have the x-axis as axis of symmetry; they have reflection symmetry with respect to the equatorial plane. We shall see in Section 4 that in many cases these models are prolate.

The gravitational potential V_S of a mass model defined by (16) is given by

$$V_S = g_\lambda U(\lambda) + g_\mu U(\mu) = -\frac{(\lambda+\alpha)G(\lambda)-(\mu+\alpha)G(\mu)}{\lambda-\mu}, \tag{18}$$

with

$$U(\tau) = -G(\tau) = -2\pi G\Psi(\infty) + \frac{2\pi G}{\sqrt{|\tau+\alpha|}}\int_{-\alpha}^{\tau}\frac{\sqrt{|\sigma+\alpha|}}{2(\sigma+\beta)}\Psi(\sigma)\,d\sigma. \tag{19}$$

The expression for the total mass is given in equation (41) of Paper II.

We remark that, whereas here we define a completely separable mass model by a specification of its density profile in the equatorial plane, it is, in this special case of $\gamma=\beta$, also possible to define it by giving the circular velocity as function of radius in this plane. An early example was given by Lynden-Bell (1960).

2.3 PROLATE SPHEROIDAL COORDINATES

For $\beta=\alpha$ we have $\Delta_1=\Delta_2$ and the ellipsoidal coordinates reduce to prolate spheroidal coordinates (λ, ϕ, ν), with the z-axis as symmetry axis (Paper I). Let (ϖ, z, ϕ) be cylindrical coordinates with $\varpi^2=x^2+y^2$. In each meridional plane $\phi=$constant, λ and ν are elliptic coordinates with foci at $\varpi=0$, $z=\pm\Delta_2$.

Upon taking $\mu=-\beta=-\alpha$, equation (3) defines an axisymmetric mass model with (given) z-axis density profile $\psi(\tau)\,(z^2=\tau+\gamma;\ \tau=\lambda, \nu)$. The expression for the density $\varrho(\lambda, \nu)$ at a general point in terms of $\psi(\tau)$ was first derived by Kuzmin (1956). It is

$$\varrho(\lambda, \nu) = g_\lambda^2\psi(\lambda) + 2g_\lambda g_\nu\frac{[\Psi(\lambda)-\Psi(\nu)]}{\lambda-\nu} + g_\nu^2\psi(\nu), \tag{20}$$

with

$$g_\lambda = \frac{\lambda+\alpha}{\lambda-\nu}, \qquad g_\nu = \frac{\nu+\alpha}{\nu-\lambda}. \tag{21}$$

A choice of Δ_2 defines a prolate spheroidal coordinate system. It follows that for a given density profile $\psi(z)$ there exists a *one-parameter family* of mass models that have a potential of Stäckel form in these coordinates. All these models have the z-axis as axis of symmetry; they have reflection symmetry with respect to the equatorial plane. We shall see in Section 4 that in many cases these mass models are oblate.

The gravitational potential V_S of a mass model defined by (20) is given by

$$V_S = g_\lambda U(\lambda) + g_\nu U(\nu) = -\frac{(\lambda+\gamma)G(\lambda)-(\nu+\gamma)G(\nu)}{\lambda-\nu}, \tag{22}$$

with

$$G(\tau) = 2\pi G\Psi(\infty) - \frac{2\pi G}{\sqrt{\tau+\gamma}}\int_{-\gamma}^{\tau}\frac{(\sigma+\alpha)}{2(\sigma+\gamma)^{3/2}}\Psi(\sigma)\,d\sigma. \tag{23}$$

The total mass, M, of a model is given by

$$M=2\pi\int_{-\gamma}^{\infty}\frac{(\sigma+2\gamma-\alpha)}{\sqrt{\sigma+\gamma}}\psi(\sigma)\,d\sigma=4\pi\int_{0}^{\infty}(z^2+\Delta_2^2)\,\psi(z)\,dz. \tag{24}$$

It should be noted that the mass models defined by (16) and (20) – for the same $\psi(\tau)$ – are different. The former have the z-axis as symmetry axis, whereas the latter have the x-axis as axis of symmetry. However, *in each of the meridional planes their density distributions are identical.* As a result, many properties of the models defined by (20) can be deduced immediately from those defined by (16) by taking μ and β instead of ν and γ, respectively, in the appropriate equations. The density distributions in these meridional planes are also valid for the principal planes of the triaxial models, as is clear from a comparison with equations (6), (7) and (9).

3 Elementary densities

In order to experiment with the use of equation (3), we consider densities on the z-axis that are delta-functions. The resulting separable densities will be called *elementary densities*. Any density profile $\psi(z)$ may be represented as an integral over delta-functions. The complete separable mass model that belongs to $\psi(z)$, for a chosen coordinate system, then is the same integral over the elementary densities.

3.1 ELLIPSOIDAL COORDINATES

For $\psi(z)=\delta(z-z_0)$ we have

$$\psi(\tau)=2\sqrt{\tau_0+\gamma}\,\delta(\tau-\tau_0), \tag{25}$$

where $z_0^2=\tau_0+\gamma$. Since, by assumption, $\psi(-z)=\psi(z)$, the density (25) corresponds to *two* delta-function densities, one at $z=z_0$, and the other at $z=-z_0$. The shape of the density distribution depends on the position of the points defined by $\tau=\tau_0$ with respect to the foci on the z-axis, i.e. it depends on the value of Δ_1 and Δ_2. We briefly discuss the different cases. They are illustrated in Fig. 1.

When $\Delta_2\leq z_0$ the delta-function densities are beyond the outer foci on the z-axis. We write $\tau_0=\lambda_0$, and find

$$\varrho(\lambda,\mu,\nu)=2\sqrt{\lambda_0+\gamma}\left[2g_\lambda\left(\frac{g_\mu}{\lambda-\mu}+\frac{g_\nu}{\lambda-\nu}\right)H(\lambda-\lambda_0)+g_\lambda^2\delta(\lambda-\lambda_0)\right], \tag{26}$$

where H is the Heavyside function. The elementary density (26) is zero inside the ellipsoid $\lambda=\lambda_0$, infinite on it, and falls off as r^{-4} at large radii (Fig. 1a). When $z_0=\Delta_2$, i.e. $\tau_0=-\alpha$, the density (26) is infinite on the ellipse $y^2/(\beta-\alpha)+z^2/(\gamma-\alpha)=1$ in the (y, z)-plane, zero for $\lambda=-\alpha$ in this plane, and non-zero outside it (Fig. 1b).

For $\Delta_1\leq z_0\leq\Delta_2$ the delta-function densities are between the inner and outer foci on the z-axis. In this case $\tau_0=\mu_0$, and

$$\varrho(\lambda,\mu,\nu)=2\sqrt{\mu_0+\gamma}\left[2g_\lambda\left(\frac{g_\mu}{\lambda-\mu}+\frac{g_\nu}{\lambda-\nu}\right)H(\mu_0-\mu)\right.$$
$$\left.+2g_\nu\left(\frac{g_\lambda}{\lambda-\nu}+\frac{g_\mu}{\lambda-\mu}\right)H(\mu-\mu_0)+g_\mu^2\delta(\mu-\mu_0)\right]. \tag{27}$$

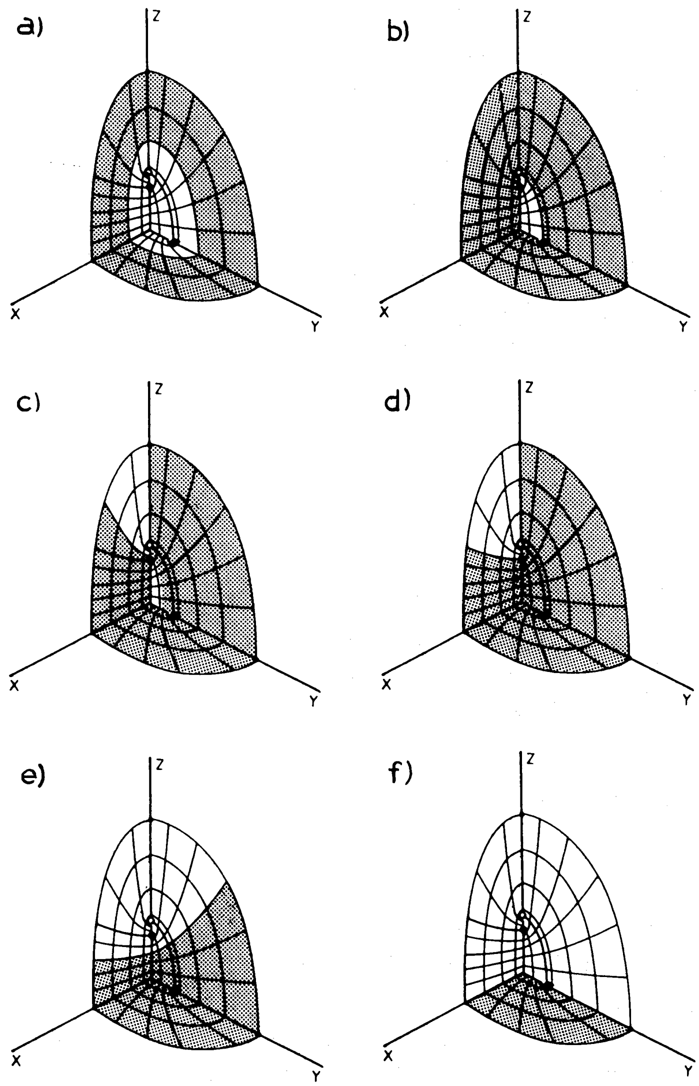

Figure 1. Elementary density distributions for the triaxial case. Shading indicates a non-zero density. The three pairs of foci are denoted by the open and filled circles and the filled squares. Further details are given in the text. (a) $\Delta_2 < z_0$, (b) $z_0 = \Delta_2$, (c) $\Delta_1 < z_0 < \Delta_2$, (d) $z_0 = \Delta_1$, (e) $0 < z_0 < \Delta_1$, (f) $z_0 = 0$.

This density is infinite on the hyperboloid of one sheet $\mu = \mu_0$, zero for $\lambda = -\alpha$ and $\mu < \mu_0$ in the plane $x = 0$, also zero for $\nu = -\beta$ and $\mu > \mu_0$ in the plane $y = 0$, and non-zero everywhere else (Fig. 1c). Since $\lambda \sim r^2$ at large radii r, the mass in a spherical shell with inner radius r and outer radius $r + dr$ decreases proportional to r^{-2} at large radii. For $z_0 = \Delta_1$ the density is infinite on the two branches of the hyperbola $x^2/(\alpha - \beta) + z^2/(\gamma - \beta) = 1$ in the (x, z)-plane, zero for $\nu = -\beta$ in this plane, and non-zero outside it (Fig. 1d).

When $0 \leq z_0 \leq \Delta_1$ the delta-function densities on the z-axis are between the origin and the inner foci. Now $\tau_0 = \nu_0$, and we find

$$\varrho(\lambda, \mu, \nu) = 2\sqrt{\nu_0 + \gamma}\left[2g_\nu\left(\frac{g_\lambda}{\lambda - \nu} + \frac{g_\mu}{\mu - \nu}\right)H(\nu_0 - \nu) + g_\nu^2\delta(\nu - \nu_0)\right]. \tag{28}$$

In this case the density is finite between the two sheets of the hyperboloid $\nu = \nu_0$, infinite on it, and zero outside it (Fig. 1e). The mass in a spherical shell falls off as r^{-2} at large radii. When $z_0 = 0$, i.e. $\nu_0 = -\gamma$, the density (28) is an infinitesimally thin disc in the (x, y)-plane (Fig. 1f). It is identical to the *perfect elliptic disc*, discussed in detail in Paper I. This is the only disc that has a potential of three-dimensional Stäckel form in the chosen ellipsoidal coordinate system.

The gravitational potential of the elementary densities can be calculated easily. For an elementary density outside the outer foci [*cf.* (26)] the potential is constant inside the ellipsoid $\lambda=\lambda_0$, where the density is zero.

From the properties of the elementary densities it is evident that a large variety of triaxial mass models with Stäckel potentials must exist. If the chosen $\psi(z)$ is such that the z-axis density is relatively large between the centre and the inner foci, the corresponding mass model has a high density close to the (x, y)-plane, and will tend to be rather flattened. In the case where $\psi(z)$ is relatively large between the inner and the outer foci, the density around the x-axis is high, and the model will tend to be elongated in this direction. A large density on the z-axis beyond the outer foci results in a model with most of its mass at large radii. Here the ellipsoids of constant λ are nearly round, so that the model will be nearly spherical.

At large radii, the elementary densities are either zero, or they fall off as r^{-4} (in the sense that the mass in a spherical shell decreases as r^{-2}). It follows that, if $\psi(z)\simeq z^{-s}$ for large z, then in all other directions

$$\begin{aligned}\varrho(\lambda, \mu, \nu) &\sim r^{-s} \qquad \text{for } s<4,\\ &\sim r^{-4} \qquad \text{for } s\geq 4.\end{aligned} \tag{29}$$

As a result, *the separable density* $\varrho(\lambda, \mu, \nu)$ *that corresponds to a given* $\psi(z)\geq 0$ *cannot fall off more rapidly than* r^{-4} *as* $r\to\infty$, *except on the* z*-axis*. Thus, mass models with a Stäckel potential in which $\psi(z)$ decreases faster than z^{-4} as $z\to\infty$ are somewhat artificial.

We remark that density distributions with a Stäckel potential in which $\psi(z)\to\infty$ for $z\to 0$ must have $\varrho\to\infty$ in the whole (x, y)-plane. Models with a Stäckel potential in ellipsoidal coordinates and a singular density in the centre only do not exist.

3.2 PROLATE SPHEROIDAL COORDINATES

In the limit $\beta=\alpha$ the expressions for the elementary densities derived in Section 3.1 become somewhat simpler. When $\Delta_2\leq z_0$ we have $\tau_0=\lambda_0$ and Kuzmin's formula (20) gives

$$\varrho(\lambda, \nu)=2\sqrt{\lambda_0+\gamma}\left[\frac{2g_\lambda g_\nu}{\lambda-\nu}H(\lambda-\lambda_0)+g_\lambda^2\delta(\lambda-\lambda_0)\right]. \tag{30}$$

This elementary density is illustrated in Fig. 2(a). The density is zero inside the prolate spheroid $\lambda=\lambda_0$. On the spheroid it is infinite, and it falls off as r^{-4} at large distances from the centre.

When $0\leq z_0\leq\Delta_2$, we have $\tau_0=\nu_0$ and find

$$\varrho(\lambda, \nu)=2\sqrt{\nu_0+\gamma}\left[\frac{2g_\lambda g_\nu}{\lambda-\nu}H(\nu_0-\nu)+g_\nu^2\delta(\nu-\nu_0)\right]. \tag{31}$$

This density is finite between the two sheets of the hyperboloid of revolution $\nu=\nu_0$, infinite on the hyperboloid, and zero outside it (Fig. 2b). At large radii the density falls off as r^{-4}. For $z_0=0$ it reduces to an infinitesimally thin disc in the (x, y)-plane, which is identical to Kuzmin's disc (Kuzmin 1953; Paper I). When $z_0=\Delta_2$ the delta-function densities are at the two foci. In this case the elementary density is everywhere non-zero and is infinite only at the foci.

The gravitational potential of two point masses is separable in prolate spheroidal coordinates that have their foci at the positions of the point masses. This was demonstrated by Jacobi (1839; 1866) in his re-derivation of Euler's (1760) solution of the famous problem of motion in the

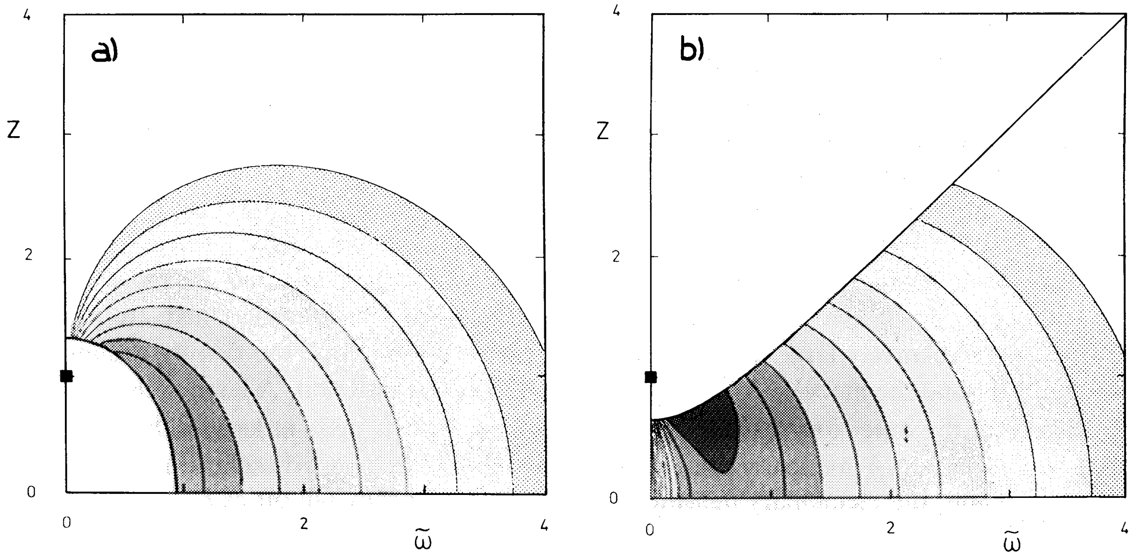

Figure 2. Elementary density distributions. Densities are indicated by the grey scale. Contour values are logarithmically spaced, with intervals of log 1.62. The thick black curve is the bounding coordinate line ($\tau=\tau_0$) where the density is a delta-function. The black square indicates the position of the focus, at $z=\Delta_2$, (a) $\Delta_2<z_0$, (b) $\Delta_2>z_0$.

potential of two fixed point masses. This case was not recovered in the above analysis, because the elementary densities (30) and (31) are defined by means of Kuzmin's formula which has been derived for potentials of the form (22) with $G(\tau)$ continuous at $\tau=-\alpha$. The potential of two point masses, M, in the foci is indeed of the form (22), but with $G(\lambda)=2GM/\sqrt{\lambda}$ and $G(\nu)\equiv 0$, so that in this case $G(\tau)$ is not a continuous function of τ, and Kuzmin's formula does not apply.

From the properties of the elementary densities it follows (*cf.* Section 3.1) that mass models with a large density on the z-axis between the centre and the foci will tend to be rather flattened (i.e. oblate). If $\psi(z)$ is relatively large outside the foci, the corresponding models will be nearly spherical. The behaviour of $\varrho(\lambda, \nu)$ at large radii is identical to that given in (29) for the general case.

3.3 OBLATE SPHEROIDAL COORDINATES

In this case elementary densities are defined as the separable densities that belong to $\psi(\tilde{z})=\delta(\tilde{z}-\tilde{z}_0)$ with $\tau_0+\beta=\tilde{z}_0^2$. Expressions for $\varrho(\lambda, \mu)$ are similar to equations (30) and (31). The cross-sections of the densities with the meridional plane are identical to those illustrated in Fig. 2, if we read $(\chi, \tilde{z})$ instead of (ϖ, z).

For a relatively large density $\psi(\tilde{z})$ inside the circle $\tilde{z}=\sqrt{\beta-\alpha}$ in the equatorial plane, the corresponding separable mass model has most of its density close to the x-axis, and will tend to be elongated (i.e. prolate). When $\psi(\tilde{z})$ is relatively large outside this circle the model will be nearly round. The behaviour of $\varrho(\lambda,\mu)$ at large radii is identical to that given in (29) for the triaxial case.

4 Expansions near the centre

4.1 DENSITY

If both $\psi(-\gamma)$ and $\psi'(-\gamma)$ are finite, we can expand the density (3) around the centre in powers of x^2, y^2 and z^2, i.e.

$$\varrho(x^2, y^2, z^2)=\varrho_0\left\{1-\frac{x^2}{a_1^2}-\frac{y^2}{a_2^2}-\frac{z^2}{a_3^2}-\dots\right\}, \tag{32}$$

where we have omitted terms of order four and higher. Thus, very close to the centre, the surfaces of constant density are approximately ellipsoidal. We now relate the values of the semi-axes a_1, a_2 and a_3 to the density profile $\psi(z)$.

Close to the origin, which is at $(\lambda, \mu, \nu)=(-\alpha, -\beta, -\gamma)$, we have

$$\lambda=-\alpha+x^2+\ldots, \qquad \mu=-\beta+y^2+\ldots, \qquad \nu=-\gamma+z^2+\ldots. \tag{33}$$

By expansion of $\psi(\tau)$ and use of (3) we find

$$\varrho(x^2, y^2, z^2)=\psi(-\gamma)+\frac{2x^2}{(\gamma-\alpha)^2}\int_{-\gamma}^{-\alpha}[\psi(\sigma)-\psi(-\gamma)]\,d\sigma$$

$$+\frac{2y^2}{(\gamma-\beta)^2}\int_{-\gamma}^{-\beta}[\psi(\sigma)-\psi(-\gamma)]\,d\sigma+\psi'(-\gamma)\,z^2+\ldots. \tag{34}$$

Thus, the density very close to the centre is determined by the *complete* z-axis density profile between the centre and the foci, in agreement with the properties of the elementary densities discussed in Section 3.1. The axis ratios of the ellipsoidal surfaces of constant density near the centre follow from

$$\frac{a_3^2}{a_1^2}=\frac{2}{(\gamma-\alpha)^2}\times\frac{1}{\psi'(-\gamma)}\int_{-\gamma}^{-\alpha}[\psi(\sigma)-\psi(-\gamma)]\,d\sigma,$$

$$\frac{a_3^2}{a_2^2}=\frac{2}{(\gamma-\beta)^2}\times\frac{1}{\psi'(-\gamma)}\int_{-\gamma}^{-\beta}[\psi(\sigma)-\psi(-\gamma)]\,d\sigma. \tag{35}$$

This shows explicitly that for a fixed function $\psi(z)$ the values of $\Delta_2=\sqrt{\gamma-\alpha}$ and $\Delta_1=\sqrt{\gamma-\beta}$ determine the values of a_3/a_1 and a_3/a_2, respectively.

When $\beta=\alpha$ the ellipsoidal coordinates reduce to prolate spheroidal coordinates, and we obtain $a_2=a_1$, in agreement with the fact that in this case the separable mass models have the z-axis as axis of symmetry. In case $\gamma=\beta$, the mass models have a potential of Stäckel form in oblate spheroidal coordinates, and $a_2=a_3$.

In the limit $\gamma=\beta=\alpha$ we obtain $a_3=a_2=a_1$. Thus, as the coordinate system becomes spherical, the equidensity surfaces near the centre are spheres, irrespective of the form of $\psi(z)$. This is as it should be, since the only potentials separable in spherical coordinates that give rise to non-singular densities are themselves spherical. As a result, when $\gamma=\beta=\alpha$ the whole mass model is spherical.

The surfaces of constant λ are triaxial ellipsoids with the short axis in the x-direction, and the long axis in the z-direction ($\alpha<\beta<\gamma$). Eddington (1915) conjectured that the surfaces of constant density in a mass model with a Stäckel potential would always be elongated most in the x-direction, and least in the z-direction, so that $a_1>a_2>a_3$. In particular, this would mean that mass models with a potential of Stäckel form in *prolate* spheroidal coordinate would always be *oblate*, and vice versa. It follows from (35), however, that this is not true. It is not difficult to find functions $\psi(\tau)$ such that a_1, a_2 and a_3 do *not* satisfy the inequality $a_1>a_2>a_3$. We shall give an example in Section 6. However, if both $\psi(\tau)$ and $|\psi'(\tau)|$ are *monotonically decreasing functions of τ for $-\gamma\leq\tau\leq-\alpha$, then $a_1>a_2>a_3$.*

4.2 POTENTIAL

The potential V_S can be expanded around the centre as

$$V_S=V_0+V_1x^2+V_2y^2+V_3z^2+V_{11}x^4+2V_{12}x^2y^2+2V_{13}x^2z^2+V_{22}y^4+2V_{23}y^2z^2+V_{33}z^4+\ldots. \tag{36}$$

By expansion of $G(\tau)$ around $-\alpha$, $-\beta$ and $-\gamma$, and use of (33), we obtain

$$V_0=U(-\gamma), \qquad V_1=\frac{U(-\alpha)-U(-\gamma)}{\gamma-\alpha}, \qquad V_2=\frac{U(-\beta)-U(-\gamma)}{\gamma-\beta}, \qquad V_3=U'(-\gamma). \quad (37)$$

Explicit expressions for the special values of $U(\tau)$ and $U'(\tau)$ in terms of $\psi(\tau)$ can be found by means of the equations given in Paper II, and relation (12). The coefficients of the higher order terms can be derived in the same way. They are most conveniently expressed in terms of the lower order coefficients. We find

$$V_{12}=2\,\frac{(V_1-V_2)}{(\beta-\alpha)}, \qquad V_{13}=2\frac{(V_1-V_3)}{(\gamma-\alpha)}, \qquad V_{23}=2\frac{(V_2-V_3)}{(\gamma-\beta)}, \quad (38)$$

and

$$3V_{11}+V_{12}+V_{13}=4\pi G\,\frac{[\Psi(-\alpha)-(\gamma-\alpha)\,\psi(-\gamma)]}{(\gamma-\alpha)^2},$$

$$V_{12}+3V_{22}+V_{23}=4\pi G\,\frac{[\Psi(-\beta)-(\gamma-\beta)\,\psi(-\gamma)]}{(\gamma-\beta)^2},$$

$$V_{13}+V_{23}+3V_{33}=2\pi G\psi'(-\gamma). \quad (39)$$

The expressions (39) follow also by application of Laplace's operator to the expansion (36) and comparison of the result with $4\pi G$ times the expansion (34) for the density. Poisson's equation furthermore gives

$$V_1+V_2+V_3=2\pi G\varrho_0. \quad (40)$$

In the limit $\beta=\alpha$ we find $V_1=V_2$, $V_{11}=V_{22}=½V_{12}$, $V_{13}=V_{23}$, ..., as expected. With the help of equation (23) we obtain for this case

$$\frac{V_3}{V_1}=1+3\,\frac{\int_{-\gamma}^{-\alpha} h(\sigma)[\psi(-\gamma)-\psi(\sigma)]\,d\sigma}{\int_{-\gamma}^{-\alpha} h(\sigma)\,\psi(\sigma)\,d\sigma}, \quad (41)$$

where the function $h(\sigma)$ is given in equation (A16) of Paper II, and we have used the relation

$$\int_{-\gamma}^{-\alpha} h(\sigma)\,d\sigma=-\tfrac{2}{3}(\gamma-\alpha)^{3/2}.$$

For $-\gamma\leq\tau\leq-\alpha$ we have $h(\tau)\leq 0$, so that $V_3/V_1\geq 1$, i.e. the equipotential surfaces near the centre are oblate spheroids, if $\psi(\tau)\leq\psi(-\gamma)$ for all $\tau\leq-\alpha$. This is true even if $|\psi'(\tau)|$ is not a decreasing function of τ, so that near the centre the surfaces of constant density are prolate (*cf.* Section 4.1). We conclude that *for all centrally concentrated mass models for which the equations of motion separate in prolate spheroidal coordinate the potential is oblate.*

In the limit $\gamma=\beta$ we have $V_2=V_3$, $V_{22}=V_{33}=½V_{23}$, $V_{12}=V_{13}$, etc. We now find

$$\frac{V_2}{V_1}=1+\frac{3}{2}\,\frac{\int_{-\beta}^{-\alpha} h(\sigma)[\psi(-\beta)-\psi(\sigma)]\,d\sigma}{\int_{-\beta}^{-\alpha} h(\sigma)\,\psi(\sigma)\,d\sigma}, \quad (42)$$

where in this case $h(\sigma)$ is given in equation (A14) of Paper II, and

$$\int_{-\beta}^{-\alpha} h(\sigma)\,d\sigma=\frac{1}{3}(\beta-\alpha)^{3/2}.$$

As long as $\psi(-\beta)\geq\psi(\tau)$ for $-\beta\leq\tau\leq-\alpha$ (so that the density in the equatorial plane between the centre and the focal circle $\tilde{z}=\Delta_2$ is decreasing) we have $V_2/V_1\geq 1$, so that near the centre the equipotential surfaces are prolate spheroids. It follows that *for all centrally concentrated mass models for which the equations of motion separate in oblate spheroidal coordinates, the potential is prolate*.

In a similar way we can calculate V_3/V_1 and V_3/V_2 for the triaxial models. The resulting expressions are lengthy combinations of complete elliptic integrals of the first and second kinds. We conjecture that $V_3>V_2>V_1$ for all centrally concentrated mass models with a Stäckel potential, so that the potential is elongated most along the x-axis and least along the z-axis, just as the density. By contrast, the surfaces of contant λ are elongated least along the x-axis, and most along the z-axis.

5 A specific family of models

5.1 DEFINITION

We now consider the separable mass models that belong to a simple set of smooth z-axis density profiles, for which the required integrations can be carried out mainly by analytic means. We take

$$\psi(z)=\frac{\varrho_0 c^s}{(z^2+c^2)^{s/2}}, \tag{43}$$

for various values of $s>0$ (c is a constant). The central density is ϱ_0. At large distances from the centre $\psi(z)$ decreases to zero proportional to z^{-s}. For $s=5$ the profile (43) is that of a Plummer (1911) model. For $s=3$ the function (43) is the (modified) Hubble profile, with core radius, c. Radial profiles like this are often used to model elliptical galaxies (e.g. Schwarzschild 1979). A spherical model with $s=2$ has a logarithmic potential and hence has a rotation curve that is asymptotically flat at large radii.

5.2 DENSITY

On the z-axis we have $z^2=\tau+\gamma\,(\tau=\lambda,\mu,\nu)$. Without loss of generality we choose $\gamma=-c^2$ so that (43) becomes

$$\psi(\tau)=\frac{\varrho_0 c^s}{\tau^{s/2}}. \tag{44}$$

Its primitive function [*cf.* (4)] is:

$$\begin{aligned}\Psi(\tau)&=\frac{2\varrho_0 c^2}{2-s}\left[\frac{c^{s-2}}{\tau^{(s-2)/2}}-1\right], && s\neq 2,\\ &=\varrho_0 c^2(\ln\tau-\ln c^2), && s=2.\end{aligned} \tag{45}$$

For each choice of ellipsoidal coordinates (λ,μ,ν) the generalized Kuzmin formula (3) now determines a complete mass model. It follows from (44) that $\psi(\tau)$ and $|\psi'(\tau)|$ are monotonically decreasing functions of τ for all $\tau\geq-\gamma$. As a result, for all positive values of Δ_1 and Δ_2 we find a triaxial mass model with surfaces of constant density that are all elongated most in the x-direction and least in the z-direction, a short-axis density profile (43), and a gravitational potential of Stäckel form. This is true for all values of $s>0$.

The axis ratios a_3/a_1 and a_3/a_2 of the surfaces of constant density near the centre can be calculated by means of (35). We find

$$\begin{aligned}\frac{a_3^2}{a_1^2} &= \frac{4q^2}{s(s-2)(q^2-1)^2}(2q^s - sq^2 + s - 2), \qquad s\neq 2,\\ &= \frac{2q^2}{1-q^2}\left(1 - \frac{4q^2}{1-q^2}\ln q\right), \qquad s=2,\end{aligned} \tag{46}$$

where we have written

$$q = \sqrt{\frac{\gamma}{\alpha}} = \frac{c}{\sqrt{c^2+\Delta_2^2}}. \tag{47}$$

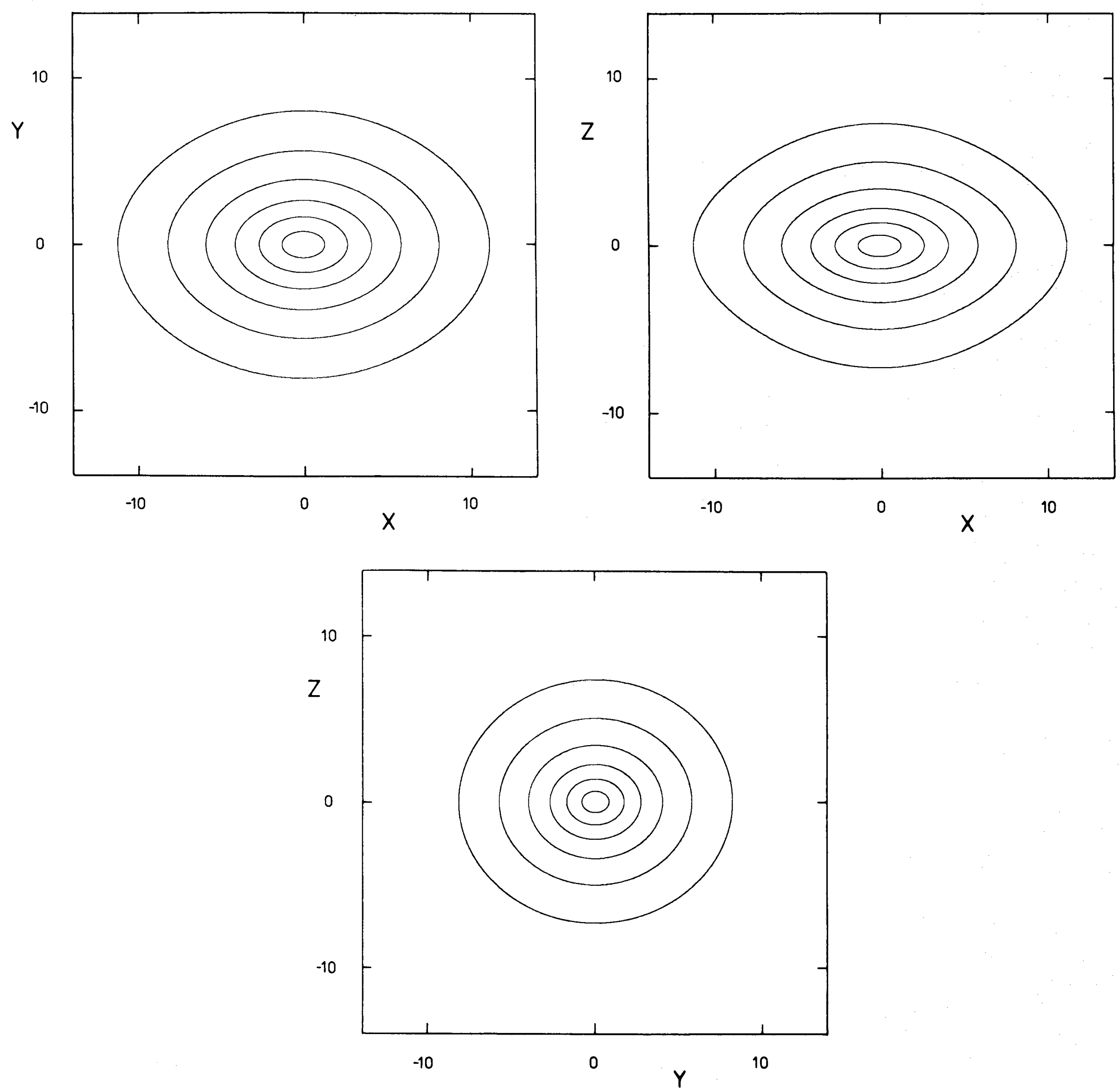

Figure 3. Contours of constant density in the principal planes of the triaxial model with the modified Hubble profile, defined by equations (44) and (45) with $s=3$, $c=1$ and central axis ratios a_1:a_2:a_3=1:0.625:0.5. Contour values are spaced logarithmically, with intervals of log 3.

The expression for a_3/a_2 is identical if we replace q by $q/p=\sqrt{\gamma/\beta}=c/\sqrt{c^2+\Delta_1^2}$ (so that $p=\sqrt{\beta/\alpha}$). We remark that, for fixed c, a_3/a_1 and a_3/a_2 may take all values between 0 and 1, by proper choice of Δ_1 and Δ_2.

The case $s=4$ deserves special attention. We find from (46) that $a_3/a_1=q$ and $a_2/a_1=p$. Equation (3) gives

$$\varrho(\lambda, \mu, \nu)=\varrho_0\left(\frac{\alpha\beta\gamma}{\lambda\mu\nu}\right)^2=\frac{\varrho_0}{(1+m^2)^2}, \qquad m^2=\frac{x^2}{a_1^2}+\frac{y^2}{a_2^2}+\frac{z^2}{a_3^2}, \tag{48}$$

and $\gamma=-c^2=-a_3^2$, $\beta=-a_2^2$, $\alpha=-a_1^2$. Thus, the surfaces of constant density are all similar, concentric ellipsoids. This model is the *perfect* ellipsoid, described in detail in Paper I.

In Fig. 3 we show contours of constant density in the three principal planes of the model with $s=3$ and central axis ratios a_1:a_2:a_3=1:⅝:½. The surfaces of constant density evidently are smooth, and nearly ellipsoidal. They become spherical as $r=\sqrt{x^2+y^2+z^2}\to\infty$. This case may be compared with Schwarzschild's (1979) triaxial density distribution which is the basis for his

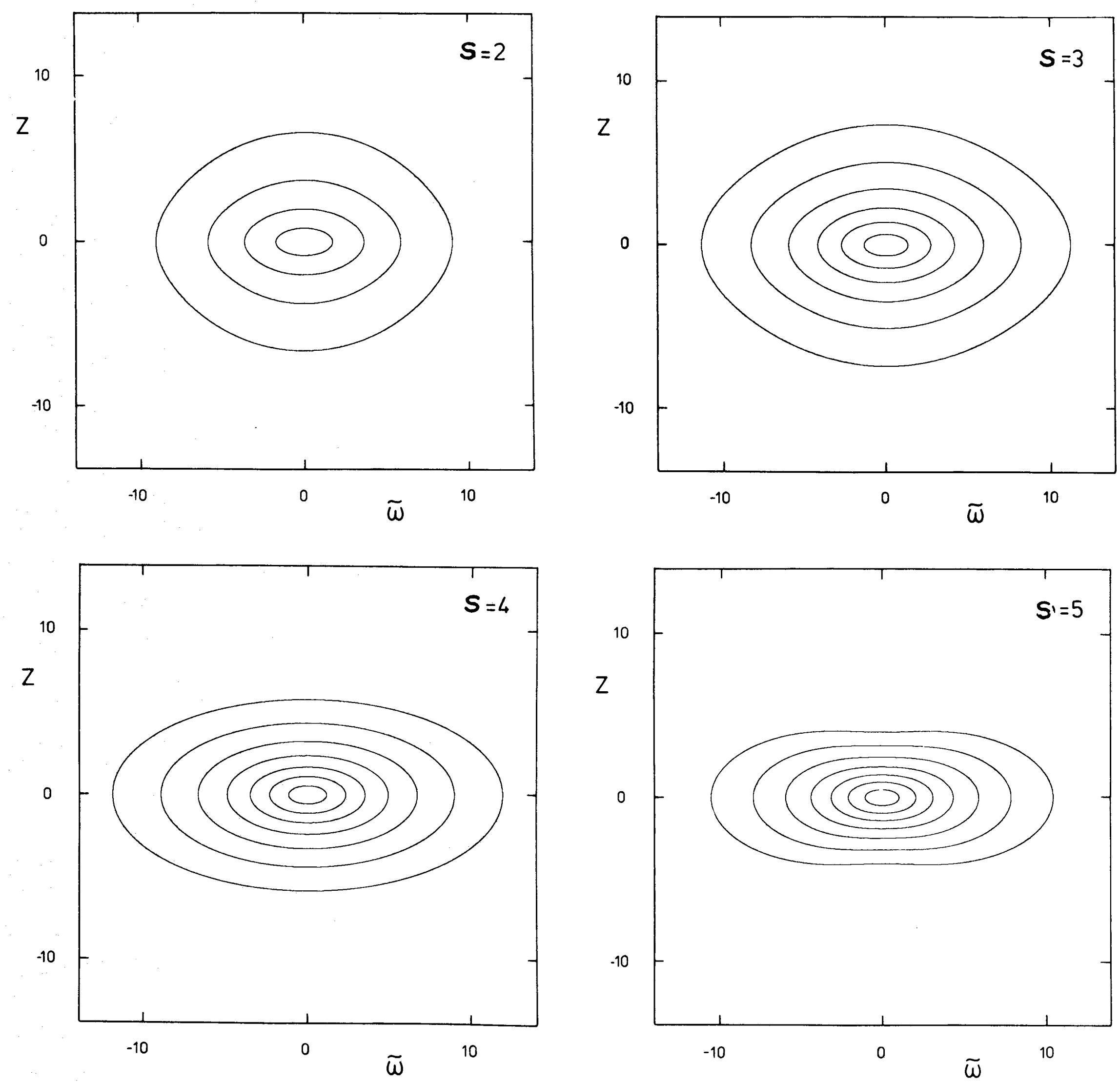

Figure 4. Contours of constant density in the meridional plane of models defined by equations (44) and (45) with s=2, 3, 4 and 5, c=1, and central axis ratio equal to 0.5. Contour values are spaced logarithmically, with intervals of log 3.

numerical construction of a self-consistent galaxy. He used a non-separable potential such that the corresponding radial density profile is $\sim(1+r^2)^{-3/2}$, and required that the axis ratios of the density are 1:⅝:½ at small *and* large radii. At intermediate distances they differ by amounts of up to 15 per cent from these values (*cf.* de Zeeuw & Merritt 1983).

Fig. 4 shows contours of constant density in the meridional plane (ϖ, z) of the oblate ($\beta=\alpha$) models with $s=2$, 3, 4 and 5, and a central axis ratio of 0.5. In Fig. 5 the ellipticity, ε, of the contours of constant density is given as function of logarithmic distance along the z-axis for a number of models. The ellipticity is defined as 1 minus the ratio of short over long axis. As we have seen in Section 2, these figures apply equally well to the density distribution in any of three principal planes of the triaxial mass models with $s=2$, 3, 4 and 5. This can be seen explicitly by a comparison of Fig. 3 with Fig. 4(b).

The perfect ellipsoid is the only triaxial mass model with a Stäckel potential that is stratified exactly on similar concentric ellipsoids (de Zeeuw & Lynden-Bell 1985). For $s\neq4$ the surfaces of constant density are therefore not all similar ellipsoids. This can be clearly seen in Figs 3 and 4.

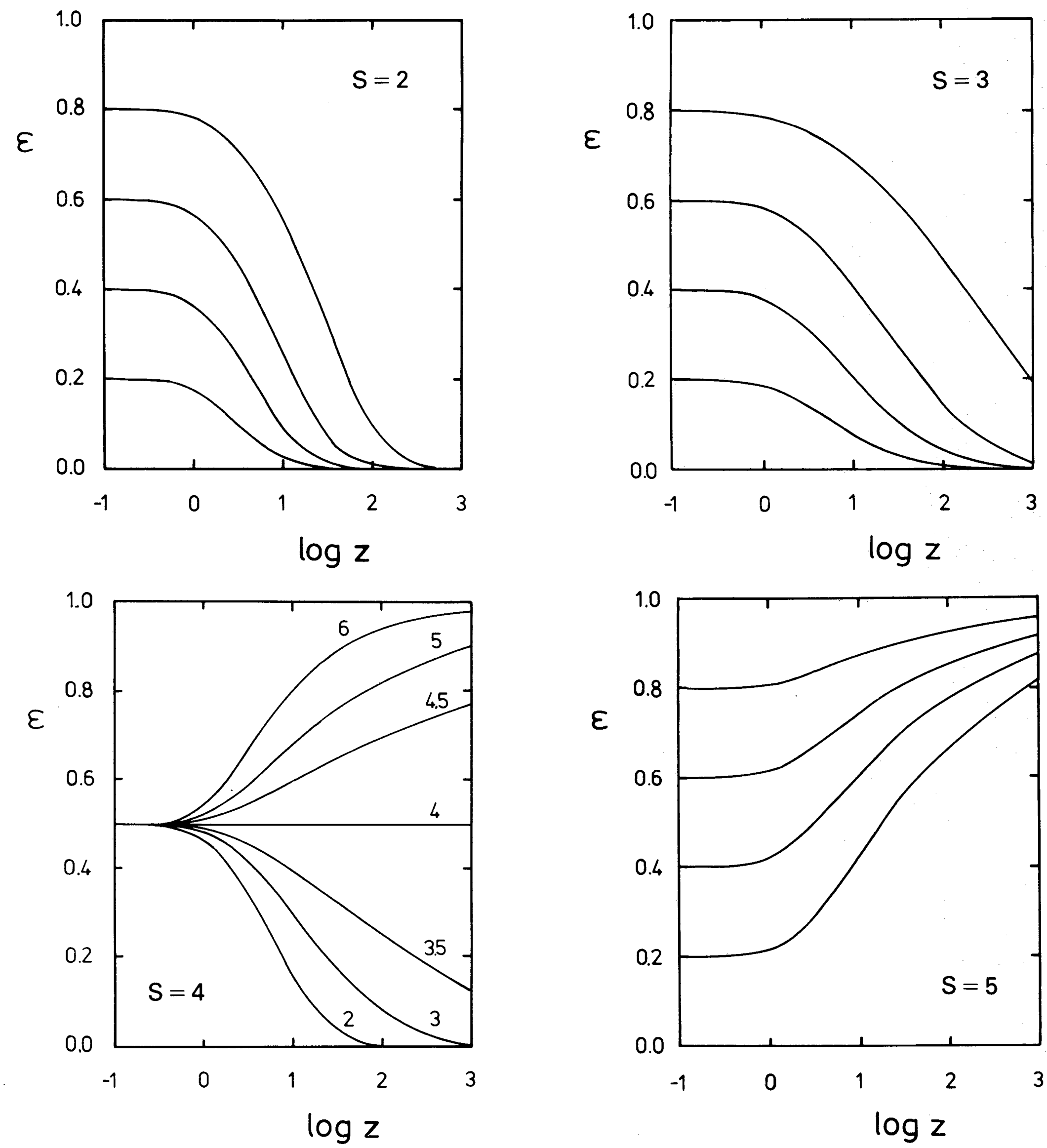

Figure 5. Ellipticity of the surfaces of constant density as function of logarithmic distance along the z-axis, for models defined by (44) and (45).

For the $s=3$ models with moderate central axis ratios – the models most relevant for elliptical galaxies – the deviations from exact ellipsoids are only of the order of a few per cent.

Models with $s<4$ become spherical in the limit $r \to \infty$. The transition occurs more rapidly for decreasing values of s (*cf*. Fig. 5). For $s>4$ the density falls off as r^{-4} in all directions, except along the z-axis. As a result, these models have equidensity surfaces that depart strongly from the nearly ellipsoidal form, with 'holes' along the z-axis, and are rather artificial. This is in agreement with our results of Section 3.

5.3 POTENTIAL

The gravitational potential of the mass models is given in equations (11) and (12), where we have to calculate $G(\tau)$ by means of equation (35) of Paper II, and use the expression (45) for $\Psi(\tau)$. For integer values of s, $G(\tau)$ can be expressed in terms of the incomplete elliptic integrals of the three kinds. The case $s=4$ is given explicitly in Appendix B of Paper I. In practice the required quadrature is most easily carried out by numerical means.

In the limit $\beta=\alpha$ all models are oblate, and the gravitational potential is given by (22) and (23). For integer values of s the function $G(\tau)$ is now elementary. Some cases of interest are

$$s=2: \quad G(\tau)=-4\pi G\varrho_0\gamma\left[\ln\left(\frac{\alpha}{\gamma}\right)-\frac{(\tau+2\gamma-\alpha)}{2(\tau+\gamma)}\ln\left(\frac{\tau}{-\gamma}\right)+\frac{(2\gamma-\alpha)}{\sqrt{-\gamma}}\left(\frac{1}{\sqrt{\tau+\gamma}}\arctan\sqrt{\frac{\tau+\gamma}{-\gamma}}-\frac{1}{\sqrt{\gamma-\alpha}}\arctan\sqrt{\frac{\gamma-\alpha}{-\gamma}}\right)\right],$$

$$s=3: \quad G(\tau)=-\frac{4\pi G\varrho_0\gamma\sqrt{-\gamma}}{\sqrt{\tau+\gamma}}\left[\ln\frac{\sqrt{\tau}+\sqrt{\tau+\gamma}}{\sqrt{-\gamma}}-\frac{(\gamma-\alpha)}{\gamma}\frac{(\sqrt{\tau}-\sqrt{-\gamma}}{\sqrt{\tau+\gamma}}\right],$$

$$s=5: \quad G(\tau)=\frac{4}{3}\pi G\varrho_0\sqrt{-\gamma}\,\frac{[(\gamma-2\alpha)\sqrt{\tau}-\alpha\sqrt{-\gamma}]}{\sqrt{\tau}(\sqrt{-\gamma}+\sqrt{\tau})}, \tag{49}$$

with, as usual, $\gamma=-c^2$. For $s=4$, see equation (27) of Paper I. We remark that for $s=2$ the potential diverges logarithmically at large radii. Instead of choosing $V_S \to 0$ as $\lambda \to \infty$ [as is done in equation (23)], we have taken $G(-\alpha)=0$ so that $V_S=0$ at the origin. For $s=3$ the total mass diverges logarithmically, but the potential is bounded.

In the limit $\gamma=\beta$ all models are prolate, and the gravitational potential is given in (18) and (19). For integer values of s the function $G(\tau)$ is again elementary. The case $s=4$ is the perfect prolate spheroid; its potential is given in equation (25) of Paper I. For $s=3$ we find

$$G(\lambda)=-\frac{4\pi G\varrho_0\beta}{\sqrt{\lambda+\alpha}}\left[\sqrt{\beta-\alpha}\arctan\sqrt{\frac{\lambda+\alpha}{\beta-\alpha}}+\sqrt{-\beta}\,\mathrm{Arth}\sqrt{\frac{\lambda+\alpha}{\lambda}}-\sqrt{\beta-\alpha}\arctan\sqrt{\frac{-\beta(\lambda+\alpha)}{(\beta-\alpha)\lambda}}\right],$$

$$G(\mu)=-\frac{4\pi G\varrho_0\beta}{\sqrt{|\mu+\alpha|}}\left[\sqrt{\beta-\alpha}\,\mathrm{Arth}\sqrt{\frac{\mu+\alpha}{\beta-\alpha}}+\sqrt{-\beta}\arctan\sqrt{\frac{|\mu+\alpha|}{\mu}}-\sqrt{\beta-\alpha}\,\mathrm{Arth}\sqrt{\frac{\beta(\mu+\alpha)}{(\beta-\alpha)\mu}}\right]. \tag{50}$$

An equivalent expression for $G(\tau)$ has been given by Gerhard & Binney (1985).

6 Other examples

In order to illustrate that the class of mass models with separable potentials is rich, we briefly consider some other simple density profiles. We restrict ourselves to models separable in prolate spheroidal coordinates. From the preceding sections it is evident that *these axisymmetric models all have triaxial counterparts with very similar properties.*

6.1 MODIFIED JAFFE MODELS

First we consider a z-axis density profile $\psi(z)$ given by

$$\psi(z)=\frac{\varrho_0 c^2}{(z^2+c^2)(z^2+1)}, \qquad 0<c^2\leq 1. \tag{51}$$

For $c=1$ this is the profile of the perfect oblate spheroid, which we already discussed in Section 5. In the limit $c\to 0$, where $\varrho_0 c^2$ is kept constant, the function (51) resembles the density profile proposed by Jaffe (1983) for elliptical galaxies. In this case $\psi(z)\sim z^{-2}$ for $z\ll 1$, and $\psi(z)\sim z^{-4}$ at

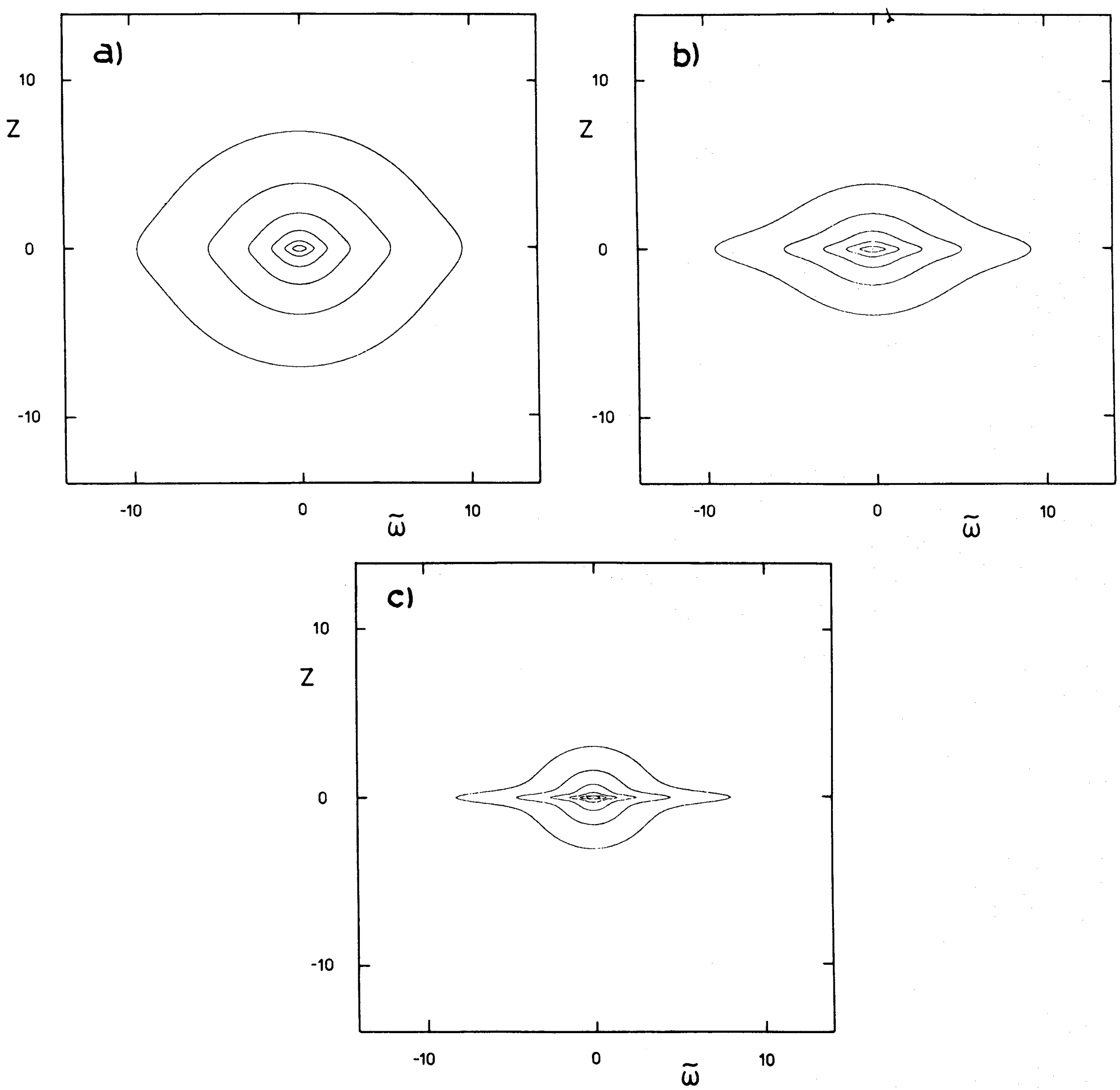

Figure 6. Contours of constant density in the meridional plane of models defined by (51) and (52). Contour values are spaced logarithmically, with intervals of log 9. (a) $\Delta_2=0.25$, $c=0.05$, (b) $\Delta_2=0.5$, $c=0.05$, (c) $\Delta_2=0.25$, $c=0.01$.

large distances from the centre. We take $c>0$ in order to avoid infinite densities in the whole equatorial plane. Nevertheless, for very small c most of the density is close to this plane. As a result, for $c \ll \Delta_2$ the mass models are strongly flattened.

In this case we have (with $\gamma=-c^2$)

$$\psi(\tau)=\frac{-\gamma\varrho_0}{\tau(\tau+\gamma+1)}, \qquad \Psi(\tau)=\frac{-\gamma\varrho_0}{\gamma+1}[\ln\tau-\ln(\tau+\gamma+1)-\ln(-\gamma)]. \tag{52}$$

Both $\psi(\tau)$ and $|\psi'(\tau)|$ are monotonically decreasing for $\tau \geq -\gamma$. All models are oblate.

The function $G(\tau)$ that via (22) defines the gravitational potential is elementary (for $\beta=\alpha$):

$$G(\tau)=-\frac{2\pi G\varrho_0\gamma}{\gamma+1}\left\{\frac{(\tau+2\gamma-\alpha)}{(\tau+\gamma)}[\ln(\tau+\gamma+1)-\ln\tau+\ln(-\gamma)]-\ln(-\gamma)\right.$$
$$\left.+\frac{(4\gamma-2\alpha)}{\sqrt{-\gamma}\sqrt{\tau+\gamma}}\arctan\sqrt{\frac{\tau+\gamma}{-\gamma}}-\frac{2(\gamma-\alpha-1)}{\sqrt{\tau+\gamma}}\arctan\sqrt{\tau+\gamma}\right\}. \tag{53}$$

The total mass, M, of the model is given by [*cf.* equation (24)],

$$M=-\frac{2\pi^2\gamma\varrho_0}{\gamma+1}\left(\frac{2\gamma-\alpha}{\sqrt{-\gamma}}+1+\alpha-\gamma\right). \tag{54}$$

It can be verified that in the limit $c \uparrow 1$ we indeed recover the results for the perfect oblate spheroid obtained in Paper I. Fig. 6 illustrates three different models.

6.2 A SIMPLE POTENTIAL

A spherical model that has been used often is the isochrone, for which many relevant quantities can be calculated explicitly by analytic means (Hénon 1959a, b, 1960; Eggen, Lynden-Bell & Sandage 1962; Mulder 1983; Binney & Petrou 1985). The spherical density distribution $\varrho(r)$ is given by

$$\varrho(r)=\frac{4\varrho_0 c^4}{3(r^2+c^2)^{3/2}}\frac{(c+2\sqrt{r^2+c^2})}{(c+\sqrt{r^2+c^2})^2}, \tag{55}$$

where c is an arbitrary constant and ϱ_0 is the central density. At large radii $\varrho(r)$ falls off as r^{-4}. We take (55) as the z-axis density profile, with again $\gamma=-c^2$, so that

$$\psi(\tau)=\frac{4\varrho_0\gamma^2}{3\tau^{3/2}}\frac{(\sqrt{-\gamma}+2\sqrt{\tau})}{(\sqrt{-\gamma}+\sqrt{\tau})^2},$$
$$\Psi(\tau)=\frac{8}{3}\varrho_0 c^3\left(\frac{1}{\sqrt{-\gamma}+\sqrt{\tau}}-\frac{1}{\sqrt{\tau}}+\frac{1}{2\sqrt{-\gamma}}\right). \tag{56}$$

For the function $G(\tau)$ we find by means of (22)

$$G(\tau)=-\frac{16}{9}\frac{\pi G\varrho_0\sqrt{-\gamma}}{\sqrt{-\gamma}+\sqrt{\tau}}\left[\gamma+2\alpha-\frac{\sqrt{-\gamma}(\gamma-\alpha)}{2(\sqrt{-\gamma}+\sqrt{\tau})}\right]. \tag{57}$$

The total mass, M, of the model is

$$M=-\frac{16}{9}\pi\varrho_0\sqrt{-\gamma}(\gamma+2\alpha), \tag{58}$$

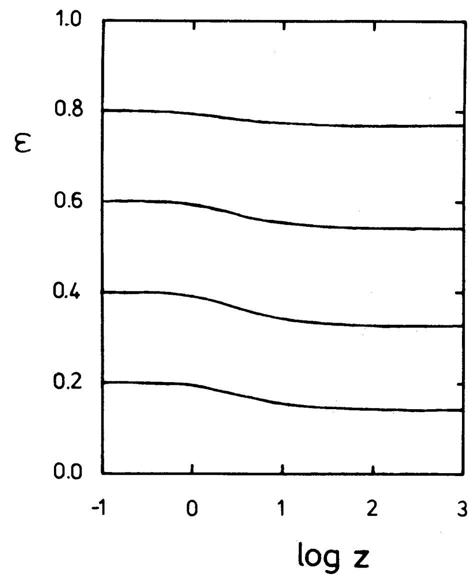

Figure 7. Ellipticity of the surfaces of constant density as function of logarithmic distance along the z-axis, for models corresponding to the simple potential (57), and $c=1$.

which is positive since $\gamma+2\alpha$ is negative. The surfaces of constant density turn out to be nearly spheroidal, with slowly varying axis ratios (Fig. 7). The central axis ratio is given by

$$\frac{a_3^2}{a_1^2}=\frac{2q^2(3+9q+q^2)}{5(1+q)^3}, \tag{59}$$

where q was defined in (47). Many other separable generalizations of the isochrone can be constructed, both axisymmetric and triaxial. An axisymmetric example with a particularly simple potential [i.e. with a function $G(\tau)$ even simpler than (57)] is given by Kuzmin (1956), and further discussed by Kuzmin & Kutuzov (1962). We shall investigate its triaxial generalization in a future paper.

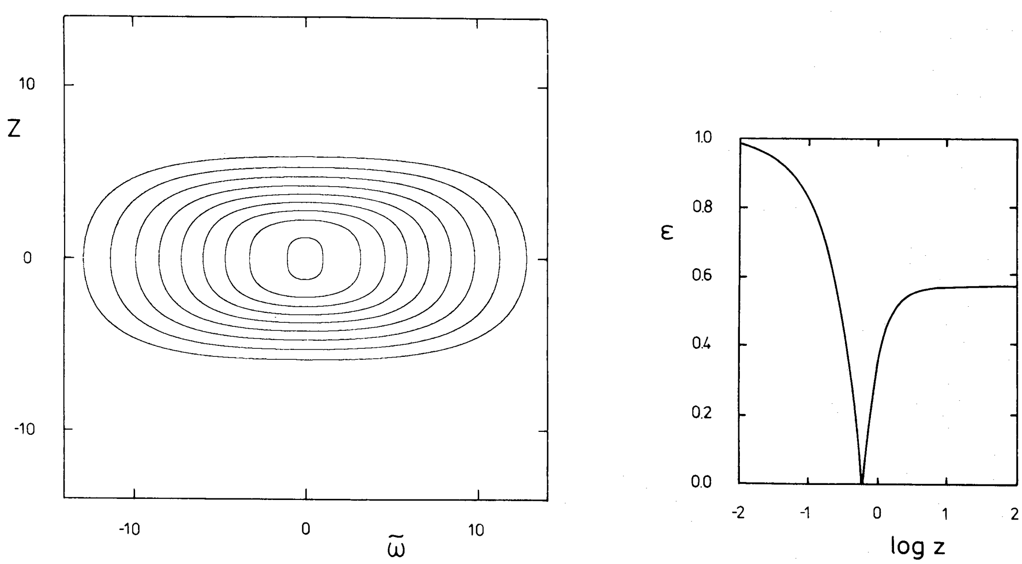

Figure 8. (a) Contours of constant density in the meridional plane of the model defined by (60) and (61), $\Delta_2=\sqrt{6.4}$, and $\gamma=-1$. Contour values are spaced logarithmically, with intervals of log 1.5. (b) Ellipticity of the surfaces of constant density as function of logarithmic distance along the z-axis of the same model. The ellipticity is defined as 1 minus the ratio of short axis over long axis. At $z=0.59$ the long and short axes exchange roles.

6.3 PROLATE/OBLATE MODELS

Another density profile is

$$\psi(z)=\frac{\varrho_0}{1+z^4}. \tag{60}$$

We find

$$\psi(z)=\frac{\varrho_0}{1+(\tau+\gamma)^2}, \qquad \Psi(\tau)=\varrho_0 \arctan(\tau+\gamma), \tag{61}$$

so that $\psi'(-\gamma)=0$. From equation (35) it follows that for all choices of prolate spheroidal coordinates – for all values of $\Delta_2>0$ – the axis ratio a_3/a_1 of the surfaces of constant density is infinite in the centre. Thus, close to the centre, these surfaces are prolate. With increasing radius the surfaces of constant density become quickly oblate, however (Fig. 8a). At large distances from the centre the density falls off as r^{-4}, and the axis ratio approaches a constant value (Fig. 8b), which is given by

$$\left(\frac{a_3}{a_1}\right)_\infty^4=\frac{1}{1+\pi(1-q^2)+(1-q^2)^2}. \tag{62}$$

The function $G(\tau)$ for this case is (for $\beta=\alpha$)

$$G(\tau)=2\pi G\varrho_0\left\{\frac{(\gamma-\alpha-1)}{\sqrt{2(\tau+\gamma)}}\ln\frac{[\tau+\gamma+\sqrt{2(\tau+\gamma)}+1]}{\sqrt{\sqrt{1+(\tau+\gamma)^2}}}+\frac{\pi}{2}\right.$$
$$\left.+\frac{(\gamma-\alpha+1)}{\sqrt{2(\tau+\gamma)}}\arccos\frac{1-(\tau+\gamma)}{\sqrt{1+(\tau+\gamma)^2}}-\frac{(\tau+2\gamma-\alpha)}{(\tau+\gamma)}\arctan(\tau+\gamma)\right\}, \tag{63}$$

and the total mass equals

$$M=\sqrt{2}(\gamma-\alpha+1)\pi^2\varrho_0. \tag{64}$$

7 Concluding remarks

It is evident that many smooth triaxial mass models with a Stäckel potential can be constructed by means of the generalized Kuzmin formula. We have obtained such models for a number of simple radial-density profiles. The models have a large variety of three-dimensional shapes.

Elliptical galaxies are unlikely to have gravitational potentials that are exactly of Stäckel form. We have not addressed the question as to how accurately one can represent these galaxies with separable mass models. From the examples presented here it follows, however, that spherical mass models that are often used to represent elliptical galaxies can be extended easily to triaxial mass models in which the equations of motion are separable. This makes it possible to investigate the dynamics of these triaxial stellar systems by essentially analytic means.

Acknowledgment

This research was supported in part by NSF Grant PHY-82-17352.

References

Binney, J. J. & Petrou, M., 1985. *Mon. Not. R. astr. Soc.*, **214**, 449.
de Zeeuw, P. T., 1985a. *Mon. Not. R. astr. Soc.*, **216**, 273, (Paper I).
de Zeeuw, P. T., 1985b. *Mon. Not. R. astr. Soc.*, **216**, 599, (Paper II).

de Zeeuw, P. T. & Lynden-Bell, D., 1985. *Mon. Not. R. astr. Soc.,* **215,** 713.
de Zeeuw, P. T. & Merritt, D. R., 1983. *Astrophys. J.,* **267,** 571.
Eddington, A. S., 1915. *Mon. Not. R. astr. Soc.,* **76,** 37.
Eggen, O., Lynden-Bell, D. & Sandage, A., 1962. *Astrophys. J.,* **136,** 748.
Euler, L., 1760. *Mem. de l'Acad. de Berlin.*
Gerhard, O. E., 1985. *Astr. Astrophys.,* **151,** 279.
Gerhard, O. E. & Binney, J. J., 1985. *Mon. Not. R. astr. Soc.,* **216,** 467.
Hénon, M., 1959a. *Annls d'Astrophys.,* **22,** 126.
Hénon, M., 1959b. *Annls d'Astrophys.,* **22,** 491.
Hénon, M., 1960. *Annls d'Astrophys.,* **23,** 474.
Jacobi, C. G. J., 1839. *J. Math.,* **19,** 309.
Jacobi, C. G. J., 1866. *Vorlesungen über Dynamik*, given at Königsberg, 1842–43. A. Clebsch, Reimer, Berlin.
Jaffe, W., 1983. *Mon. Not. R. astr. Soc.,* **202,** 995.
Kuzmin, G. G., 1953. *Tartu astr. Obs. Teated,* **1**.
Kuzmin, G. G., 1956. *Astr. Zh.,* **33,** 27.
Kuzmin, G. G., 1973. In: *Dynamics of Galaxies and Clusters*, *Materials of the All-Union Conference in Alma Ata*, p. 71, ed. Omarov, T. B., Akademiya Nauk Kazakhskoj SSR, Alma Ata.
Kuzmin, G. G. & Kutuzov, S. A., 1962. *Bull. Abastumani Astroph. Obs.,* **27,** 82.
Lynden-Bell,. D., 1960. *PhD thesis*, Cambridge University.
Lynden-Bell, D., 1962. *Mon. Not. R. astr. Soc.,* **124,** 95.
Morse, P. M. & Feshbach, H., 1953. *Methods of Theoretical Physics*, McGraw-Hill, New York.
Mulder, W., 1983. *Astr. Astrophys.,* **117,** 9.
Plummer, H. C., 1911. *Mon. Not. R. astr. Soc.,* **71,** 460.
Schwarzschild, M., 1979. *Astrophys. J.,* **232,** 236.
Schwarzschild, M., 1982. *Astrophys. J.,* **263,** 599.
Wilkinson, A. & James, R. A., 1982. *Mon. Not. R. astr. Soc.,* **199,** 171.